

# Journal of Soil Sciences and Agricultural Engineering

Journal homepage: [www.jssae.mans.edu.eg](http://www.jssae.mans.edu.eg)  
Available online at: [www.jssae.journals.ekb.eg](http://www.jssae.journals.ekb.eg)

## Desalination of Brackish Water Utilizing Air Gap Membrane Distillation at Two Different Cooling Water Levels

Abu-Zeid, M. A. E. R.<sup>1\*</sup> and X. Lu<sup>2</sup>

<sup>1</sup>Department of Agricultural Engineering, Faculty of Agriculture, Suez Canal University, Ismailia, 41522, Egypt.

<sup>2</sup>School of Material Science and Engineering.



Cross Mark

### ABSTRACT

In this work, the effect of two different cooling temperatures ( $T_c$ ) on the permeate flux ( $F_p$ ) and thermal efficiency ( $\eta$ ) of air gap membrane distillation (AGMD) module was studied experimentally. All data were described statistically in terms of means, standard error for means (SE), standard deviation (SD) and coefficient of variation (C.V.). Data were subjected to the analyses of the variance (ANOVA) and multivariate analysis to test the significant effect of different feed and designs at  $p < 0.05$ . Experiments were conducted using brackish water with salt concentration of 10000 mg/L as the feed solution under diverse hot feed temperatures ( $T_f$ ) and flow rates ( $M_f$ ). Experimental results revealed that the percentage of AGMD permeate flux was reduced by 4.71%, 4.98%, 7.51%, 1.84%, 2.71%, 8.20%, 2.25% and 4.42% at increasing cooling temperature from 10 to 20 °C, respectively, in case of flow rate ( $M_f$ ) of 2.0 and 4.0 L/m (temperature  $T_f$  of 50 °C), 6.0 and 8.0 L/m (temperature  $T_f$  of 50, 60 and 70 °C) due to lowering the temperature and vapor pressure differences between the hot and the cold feed at both sides of the membrane ( $\Delta T_{cross} = T_1 - T_4$ ). Regarding thermal efficiency ( $\eta$ ), an opposite result was obtained whereas the thermal efficiency was improved significantly at increasing cooling temperature from 10 to 20 °C at all different operating conditions. The rate of increasing in thermal efficiency were around 1.26, 1.29, 1.15 and 1.27 times at flow rate  $M_f$  of 2 L/m and different temperature  $T_f$  of 50, 60, 70 and 80 °C, respectively.

**Keywords:** Air gap membrane distillation, cooling temperature, desalination, permeate flux, thermal efficiency.

### INTRODUCTION

The problems of population explosion and climate change have obliged the specialists of the water researches at all over the world to detect alternative techniques for providing additional fresh water (Roy *et al.*, 2012; Swaminathan *et al.*, 2016). Desalination is a popular alternative process in which brackish water stream could split into fresh water or brine concentrate (Shatat *et al.*, 2013). Air gap membrane distillation (AGMD) is considered as one of the most leading membrane desalination separation processes for obtaining fresh water from brackish water at affordable cost. AGMD is characterized by minimal conduction heat loss through the hydrophobic micro-pores membrane by virtue of a sluggish air intervened between the membrane body and the cold plate (Carlsson, 1983; Andersson *et al.*, 1985; Banat, 1994).

Cooling water temperature as one of the operational parameters affecting on AGMD performance has been received a little bit concern by membrane distillation (MD) researchers. The special design for AGMD configuration; i.e. represented in presence of air gap zone; alleviated the influence of cooling temperature on AGMD permeate flux compared with other operational parameters; especially hot feed inlet temperature (Alklaibi and Lior, 2004; El-Bourawi *et al.*, 2006). This could be ascribed to low heat transfer coefficient through the air gap zone as considered a thermal insulation layer and controlled the total heat transfer coefficient in addition to the pressure of water vapor does not influence largely at these low temperatures on the cold feed side (Banat and Simandl, 1994, 1998; Alklaibi and

Lior, 2006). Reducing cooling temperature promoted comparatively the permeate flux and decreased simultaneously thermal efficiency because of increasing vapor pressure gradient. Mostly, cooling temperature is ranging from 5 to 30 °C corresponding to hot feed temperature ranging from 40 to 90 °C. In a work proceeded by Khalifa and Alawad (2018) at feed inlet temperature of 70 °C, feed salinity of 150 mg/L, feed and coolant flow rates of 2.3 L/min, the authors found that decreasing cooling temperature from 25 to 10 °C boosted the flux by 63% and 70%, respectively for series and parallel multistage AGMD modules. Khalifa *et al.* (2017) pronounced a significant flux improvement up to 63% at decreasing cooling temperature from 25 to 10 °C. Likewise, Khalifa (2018) observed that declining cooling temperature from 25 to 5 °C enhanced the AGMD permeate flux by 33% due to raising the temperature gradient across the membrane at feed temperature of 70 °C. On the other hand, Alkhudhiri *et al.* (2013) proclaimed by increasing cooling temperature from 5 °C to 25 °C, the permeate flux diminished deeply. Whereas the flux of flat sheet polytetrafluoroethylene membrane with pore size 0.2  $\mu\text{m}$  (TF200) was descended from 8.64 Kg/(m<sup>2</sup>h) (at 5 °C) to 5.04 Kg/(m<sup>2</sup>h) (at 25 °C), also the TF450 flux (pore size 0.45  $\mu\text{m}$ ) was reduced from 10.08 Kg/(m<sup>2</sup>h) to 6.12 Kg/(m<sup>2</sup>h). The reason behind low flux was because of decreasing vapor pressure difference resulted from increasing cooling temperature. Similarly, Geng *et al.* (2014) demonstrated that increasing cooling temperature from 30 to 40 °C reduced greatly the flux by about 11.1% from 3.43 to 3.05 Kg/(m<sup>2</sup>h) at feed temperature

\* Corresponding author.

E-mail address: mostafa241981@agr.suez.edu.eg

DOI: 10.21608/jssae.2020.87009

of 90 °C. Also, a reduction in flux resulted for electrospun and commercial membranes up to 32.2% and 33.6%, respectively, at increasing cooling temperature from 7 to 30 °C at constant feed temperature of 60 °C and feed flow rate of 1.5 l/min (Attia *et al.*, 2017). This attributed to decrease the driving force by increasing vapour pressure at cold feed side. Furthermore, increasing cooling temperature might decrease the condensation rate of vapour past the membrane. Meanwhile, Pangarkar and Sane (2011) stated that inconsiderable variations in flux less than 12% and 19% utilizing ground water and seawater as feed solutions, respectively by varying the cold-side temperature between 10 °C and 25 °C.

The objective of this research work is to study the the effect of two different cooling water temperatures ( $T_c$ ) on the permeate flux ( $F_p$ ), thermal efficiency ( $\eta$ ), evaporative latent heat transfer ( $Q_{lh}$ ) and energy flux ( $Q_h$ ) of air gap membrane distillation (AGMD) module using brackish water with salt concentration of 10000 mg/L as the feed.

**MATERIALS AND METHODS**

Experiments were performed at the laboratory of Institute of Biological and Chemical Engineering, State Key Laboratory of Separation Membranes and Membrane Processes, School of Material Science and Engineering, Tiangong University, Tianjin, China. These experiments were started from April 2019 to January 2020 during my work as a researcher through a postdoctoral scholarship introduced by Talent Young Scientist Program (TYSP), Beijing, China.

**AGMD experimental set-up**

The experimental set-up for the air gap membrane distillation (AGMD) system used in desalination of brackish water is shown schematically in Fig. (1). The entire AGMD system composes of feed tank, AGMD module, water pump (MP-55RZ, Shanghai Xinxishan Industrial L imited Company), heater, flow meter (LZB-4, Huanming, Yugao Industrial Automation Instrument Company, Zhejiang, China), cooler (DLSB-10, Tianjin Xingke Instrument Limited Company, China), thermostatic heating bath (Tongzhou Branch of Shanghai Jinping Instrument Limited Company, China), balance, container, and valve.

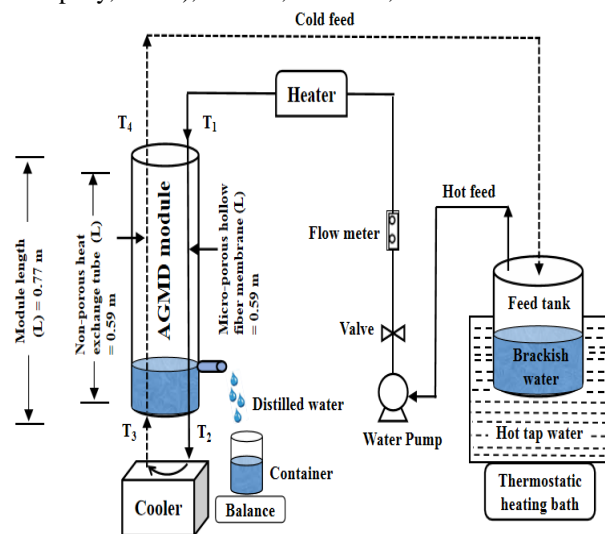


**Fig. 1. A schematic diagram showing the whole AGMD system experimental set-up**

**Materials**

The membrane module made of plexiglas and the whole AGMD system of the feed circulatory are enveloped with thermal insulation cotton to prohibit any heat loss to the environment. Non-porous polypropylene (PP) heat exchange tubes and micro-porous polyvinylidene difluoride (PVDF) hollow fibers membrane are arranged in a counter current flow. The dimensions of AGMD module used in this investigation are listed in table (1) with gap width of 5 mm.

**Table 1. Dimensions of the non-porous PP heat exchange tubes and the micro-porous PVDF hollow fibers membrane.**

Hollow fiber types	ID/OD (mm)	Number of hollow fibers	Hollow Fiber length (m)	Module length (mm)	*Inner surface area (m <sup>2</sup> )
Non-porous	0.40/0.50	240	0.59	0.77	0.18
Micro-porous	0.80/1.10	120	0.59	0.77	0.18

\*The inner surface area was estimated based on internal diameter of PVDF membrane and PP tube.

The characteristics and specifications of the PVDF hollow fibers membrane, water pump, thermostatic heating bath, and cooler are tabulated in table (2).

**Table 2. Characteristics and specifications of the PVDF hollow fibers membrane, water pump, thermostatic heating bath and cooler.**

Character	Value
PVDF hollow fibers membrane	
Thickness (µm)	150
Porosity (%)	85
pore size (µm)	0.20
Water pump (mp-55RZ Model)	
Power (KW)	0.09
Voltage (V)	220
Frequency (Hz)	50
Speed(rpm)	2800
Max. flow (L/min)	25
Highest lift (m)	10
Current (A)	0.95
Max. head (m)	8
Thermostatic heating bath (CS501 Model)	
Power (KW)	1.5
Voltage (V)	220
Frequency (Hz)	50
Highest temperature (°C)	95
Cooler (DLSB-10 Model)	
Power (KW)	0.23
Voltage (V)	220
Frequency (Hz)	50
Max. flow (L/min)	15
Highest lift (m)	10
Refrigerating capacity (KW)	0.550-0.275
Max. head (m)	3

**Experiment**

The hot feed stream was pumped from the feed tank into the hollow fibers membrane of AGMD module top in downward direction where vapor diffuses across the membrane pores. After hot feed leaving AGMD module bottom entered into cooler for necessary temperature decrease at the cold feed side. Then, after the hot feed departing cooler moved into heat exchange tubes of AGMD module bottom in an opposite direction. After cold feed leaving AGMD module top returned back to the feed tank for start a new desalination process. To maintain the feed

solution volume and feed salt concentration constant inside the feed tank throughout the experiment, the collected permeate flux (i.e., pure distilled water) returned to the feed tank. Each experiment was repeated three times under same inlet operating conditions for 1 hour operational time and average values were reported. Prior to initiating the experiment, the whole system was left running for 1 hour to guarantee no any dissolved gases in the feed stream and to reach a steady state condition.

Four different temperature sensors were fixed at the inlets and outlets of the hollow fibers membrane and the heat exchange tubes and mean temperature differences are announced due to the difficulty of measuring the interface temperature at the membrane surface. The temperature controller XMTD-3001 (Easey Commercial Building Hennessy Road Wanchai Hongkong, China) was used to control the inlet hot feed temperature. The obtained distilled water was weighted by using an electronic balance every 10 min to notice the variation of permeate flux. The electrical conductivity of distilled water and salt feed concentration are checked evermore using conductivity meter DDS-11A (Shanghai Leici Xinjing Instrument Company, China) to ensure the safety of the PVDF hollow fiber membrane and the quality of pure distilled water. A cooler was used and connected to the cold feed side of AGMD module. The module performance was investigated at different cooling temperatures ( $T_c$ ) of 10 and 20 °C, different hot feed temperatures ( $T_f$ ) of 50, 60, 70 and 80 °C, and flow rates ( $M_f$ ) of 2, 4, 6 and 8 L/m.

Thermal efficiency ( $\eta$ ) of the AGMD module can be defined as the ratio of the latent heat needed to evaporate the brackish water solution and total energy flux from the hot bulk feed across the membrane surface and air gap zone to the condensation film.  $\eta$  is calculated mathematically by (Abu-Zeid et al., 2016; Eykens et al., 2016):

$$\eta = \frac{Q_{l.h.}}{Q_h} \times 100 \quad [1]$$

Where  $Q_{l.h.}$  is the evaporative latent heat transfer through the membrane surface (MJ/h) and  $Q_h$  is the total energy flux (MJ/h) which could be determined as given by (Khayet, 2013):

$$Q_h = m_f \times C_p \times \Delta T_{drop}$$

$$Q_h = m_f \times C_p \times (T_1 - T_2) \quad [2]$$

$Q_{l.h.}$  is given by using equ. [3]:

$$Q_{l.h.} = F_p \times \Delta H_v \quad [3]$$

Where  $m$  is the feed flow rate (L/m),  $C_p$  is the specific heat of hot feed (J/kg°C),  $\Delta H_v$  is the evaporative latent heat ( $\approx 2326$  kJ/kg),  $\Delta T_{drop}$  and  $\Delta T_{cross}$  are the temperature differences alongside the hot feed channel and through the membrane (°C), respectively.  $T_1, T_2, T_3$  and  $T_4$  are the temperatures at inlet and outlet of hot bulk feed, and temperatures at inlet and outlet of cold bulk feed (°C), respectively, and  $F_p$  indicated to the permeate flux (L/(m<sup>2</sup>h)) which can be given by (Aryapratama et al., 2016):

$$F = \frac{W_w}{A \times t} \quad [4]$$

Where  $W_w$  is the mass of distilled water within time of  $t$  (kg), and  $A$  is the effective hollow fiber membrane surface area based on the internal hollow fiber diameter (m<sup>2</sup>).

The salt rejection rate (SRR) in % determined as:

$$SRR = \left( 1 - \frac{S_d}{S_f} \right) \times 100 \quad [5]$$

Where  $S_f$  is the feed salt concentration (mg/L) and  $S_d$  is the distilled water concentration (mg/L).

#### Performance evaluation

The AGMD module performance was assessed via estimating the permeate flux ( $F_p$ ) and thermal efficiency ( $\eta$ ). The specific heat ( $C_p$ ) and density ( $\rho$ ) for brackish water used in the estimation are obtained at ambient air temperature of 25 °C and listed in table (3). The various measurements of  $T_1, T_2, T_3$  and  $T_4$  are recorded every 10 min for 1 hour operational time and average values are listed in table (4) at different feed temperature ( $T_f$ ), flow rate ( $M_f$ ) and cooling temperature ( $T_c$ ).

**Table 3. The values of density ( $\rho$ ) and specific heat ( $C_p$ ) for brackish water utilized in this investigation.**

$C_f$ (mg/L)	$C_p$ (J/kg°C)	$\rho$ (kg/m <sup>3</sup> )
10000	4131.65	1004.40

**Table 4. Various temperatures of  $T_1, T_2, T_3$ , and  $T_4$  at different feed temperature ( $T_f$ ), flow rate ( $M_f$ ) and cooling temperature ( $T_c$ ).**

$T_f$ (°C)	$M_f$ (L/m)	$T_c = 10$ °C				$T_c = 20$ °C			
		$T_1$	$T_2$	$T_3$	$T_4$	$T_1$	$T_2$	$T_3$	$T_4$
50	2	57.0	20.4	10.0	38.2	54.1	26.4	20.0	38.7
	4	57.5	23.5	10.0	35.5	53.2	28.4	20.0	36.9
	6	57.5	27.0	10.0	33.0	52.9	31.2	20.0	35.4
	8	56.0	28.5	10.0	29.7	52.5	32.7	20.0	33.3
60	2	65.5	20.7	10.0	41.2	62.8	27.0	20.0	45.0
	4	66.7	25.2	10.0	39.3	63.1	31.1	20.0	44.0
	6	67.0	28.0	10.0	38.0	62.5	33.7	20.0	40.4
	8	64.9	31.5	10.0	34.5	62.2	36.4	20.0	39.7
70	2	72.5	23.6	10.0	49.9	72.2	28.2	20.0	52.7
	4	72.7	28.0	10.0	46.4	72.5	32.8	20.0	50.8
	6	72.3	31.9	10.0	43.5	71.1	35.3	20.0	47.7
	8	70.9	34.7	10.0	40.7	70.7	39.4	20.0	46.0
80	2	80.8	23.4	10.0	56.3	82.2	30.4	20.0	60.2
	4	79.6	27.2	10.0	51.7	80.8	33.8	20.0	56.3
	6	79.8	32.0	10.0	48.9	80.2	37.6	20.0	53.9
	8	78.5	35.8	10.0	47.3	80.3	41.3	20.0	53.2

**Statistical analysis**

All data were described statistically in terms of means, standard error for means (SE), standard deviation (SD) and coefficient of variation (C.V.). Data were subjected to the analyses of the variance (ANOVA) and Multivariate analysis to test the significant effect of different feed and designs at  $p < 0.05$ . The effect of studied factors (flow rate, feed temperature, cooling temperature) and their interactions on permeate flux, thermal efficiency, evaporative latent heat transfer, and energy flux were evaluated by multivariate analysis at  $p < 0.05$ . All statistical analyses were carried out using IBM-SPSS version 23.0 for Mac OS (O'Brien and Kaiser, 1985; McInnes, 2017).

**RESULTS AND DISCUSSION**

**Permeate flux ( $F_p$ )**

Figure 2(A and B) illustrated the change of AGMD permeate flux ( $F_p$ ) at cooling temperature ( $T_c$ ) varied between 10 and 20 °C and different flow rate ( $M_f$ ) of 2, 4, 6 and 8 L/m, and feed temperature ( $T_f$ ) of 50, 60, 70 and 80 °C. It was seen that the permeate flux decreased largely with increasing cooling temperature from 10 to 20 °C. This was because of lowering the temperature difference across membrane ( $\Delta T_{cross} = T_1 - T_4$ ) and a corresponding reduce in vapor pressure difference as well as low vapor condensation rate at high cooling temperature. This behaviour had appeared at some inlet operating conditions. As for example, at flow rate ( $M_f$ ) of 2 and 4 L/m under feed temperature ( $T_f$ ) of 50 °C, 6 and 8 L/m under feed temperature ( $T_f$ ) of 50, 60 and 70 °C, the percentage of flux was declined by 4.71% (2 L/m), 4.98% (4 L/m), 7.51%, 1.84%, 2.71% (6 L/m), 8.20%, 2.25%, 4.42% (8 L/m), respectively. On the contrary, at flow rate ( $M_f$ ) of 2 and 4 L/m under temperature ( $T_f$ ) of 60, 70 and 80 °C, 6 and 8 L/m under temperature ( $T_f$ ) of 80 °C, increasing cooling temperature from 10 to 20 °C improved the flux. The percentage of flux was increased by 2.80% , 3.34%, 14.78% (2 L/m), 3.18%, 3.00%, 2.64% (4 L/m), 3.19% (6 L/m), and 2.78% (8 L/m), respectively. The enhanced permeate flux taken place at cooling temperature of 10 °C compared with 20 °C interpreted by increasing  $\Delta T_{cross} = T_1 - T_4$  resulted from decreasing the outlet cold feed temperature ( $T_4$ ) at decreasing cooling temperature from 20 to 10 °C. For example, under temperature ( $T_f$ ) of 50 °C, the  $\Delta T_{cross}$  values measured at 10 °C were 18.80, 22.00, 24.70

and 26.30 °C at flow rate ( $M_f$ ) of 2, 4, 6 and 8 L/m, respectively, corresponding to only 15.40, 16.30, 17.50 and 19.20 °C at 20 °C (see table (4)).

According to multivariate statistical analysis presented in table (5) and figure 2(A and B), the main effect of  $T_f$  (50, 60, 70 and 80 °C),  $M_f$  (2, 4, 6 and 8 L/m), and cooling temperature (10 and 20 °C), and their interactions on permeate flux were assessed at  $p < 0.05$  level.  $T_f$ ,  $M_f$ , and their interaction significantly changed permeate flux ( $F = 381.3^{***}$ ,  $263.7^{***}$ ;  $11.6^{***}$ ), respectively. However, the effect of cooling temperature on permeate flux were non-significant ( $p > 0.05$ ).

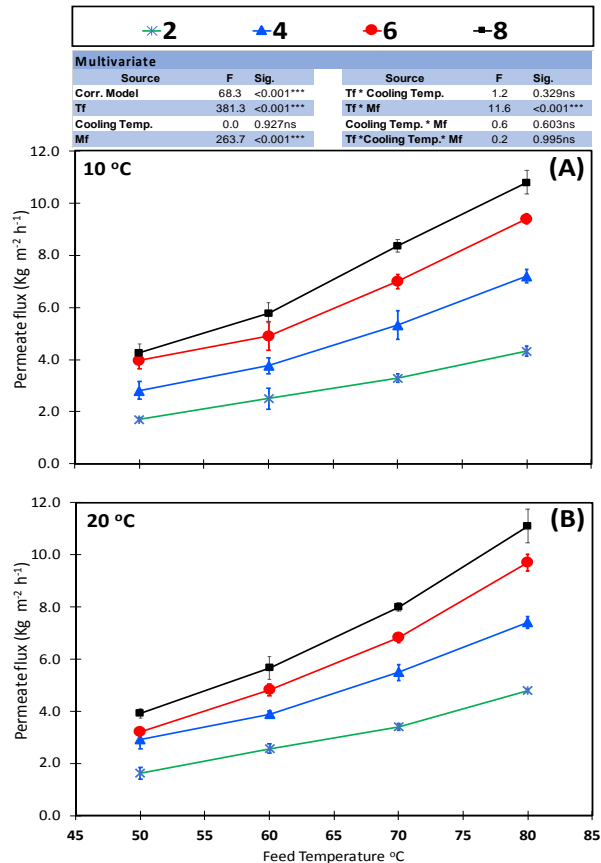


**Fig. 2. The variation of permeate flux at different feed temperature ( $T_f$ ), feed flow rate ( $M_f$ ) and cooling temperature ( $T_c$ ).**

**Table 5. Analyses of variance (ANOVA) and multivariate analysis of permeate flux at different operating conditions**

$T_f$ (°C)	$M_f$ (L/m)	Permeate flux ( $F_p$ )							
		10 °C				20 °C			
		Mean	SD	SEM	C.V.	Mean	SD	SEM	C.V.
50	2	1.70	0.11	0.06	6.55	1.62	0.38	0.22	23.15
	4	2.81	0.59	0.34	20.94	2.91	0.61	0.35	21.05
	6	3.96	0.54	0.31	13.75	3.20	0.18	0.10	5.49
	8	4.27	0.55	0.32	12.82	3.92	0.30	0.17	7.68
60	2	2.50	0.70	0.40	28.00	2.57	0.30	0.17	11.72
	4	3.77	0.53	0.31	14.15	3.89	0.20	0.12	5.12
	6	4.90	0.95	0.55	19.47	4.81	0.39	0.22	8.01
	8	5.79	0.67	0.39	11.56	5.66	0.73	0.42	12.92
70	2	3.29	0.26	0.15	7.97	3.40	0.22	0.13	6.41
	4	5.33	0.97	0.56	18.13	5.49	0.54	0.31	9.88
	6	7.00	0.48	0.28	6.89	6.81	0.29	0.17	4.21
	8	8.37	0.43	0.25	5.15	8.00	0.27	0.16	3.40
80	2	4.33	0.32	0.19	7.47	4.79	0.03	0.02	0.59
	4	7.21	0.44	0.25	6.10	7.40	0.41	0.24	5.55
	6	9.40	0.35	0.20	3.69	9.70	0.55	0.32	5.67
	8	10.80	0.80	0.46	7.41	11.10	1.12	0.64	10.06

NS; non-significant at  $p > 0.05$  \*, significant at  $p < 0.05$ ; \*\*, \*\*\* Highly significant at  $p < 0.01, 0.001$ .

**Thermal efficiency ( $\eta$ )**

Figure 3(A and B) showed the impact of varying cooling temperature on AGMD thermal efficiency ( $\eta$ ). It was found that increasing cooling temperature from 10 to 20 °C upgraded the thermal efficiency ( $\eta$ ) of AGMD module. The rate of increasing were 1.26, 1.29, 1.15, 1.27 times (2 L/m), 1.30, 1.32, 1.16, 1.14 times (4 L/m), 1.31, 1.33, 1.10, 1.15 times (6 L/m), and 1.27, 1.27, 1.11, 1.13 times (8 L/m) at different  $T_f$  of 50, 60, 70 and 80 °C, respectively. This improvement due to elevating outlet temperature of hot feed solution ( $T_2$ ) and decreasing heat loss of hot feed bulk ( $Q_h$ ) in case of cooling temperature of 20 °C compared with 10 °C. For example, under temperature ( $T_f$ ) of 50 °C, the  $T_2$  measured were 23.60, 26.20, 28.30 and 30.20 °C at  $M_f$  of 2, 4, 6, and 8 L/m, respectively, in case of cooling temperature of 20 °C, corresponding to only 19.20, 22.00, 25.00 and 26.80 °C, in case of 10 °C (see table (4)). With regard to salt rejection rate (SRR), the micro-porous PVDF hollow fibers membrane used in desalination of brackish water solution demonstrated an excellent salt separation efficiency reached up to 99.7% at different operating conditions.

Multivariate statistical analysis of thermal efficiency  $\eta$  (%) were presented in table (6) and figure 3(A and B). The main effect of  $T_f$  (50, 60, 70 and 80 °C),  $M_f$  (2, 4, 6 and 8 L/m), and cooling temperature (10 and 20 °C), and their interactions on thermal efficiency were assessed at  $p < 0.05$  level.  $T_f$ ,  $M_f$ , cooling temperature were significantly changed thermal efficiency ( $p < 0.001^{***}$ ). However, the interactions between  $T_f$ ,  $M_f$ , and cooling temperature on thermal efficiency were non-significant ( $p > 0.05$ ) as revealed by multivariate analysis of variance.

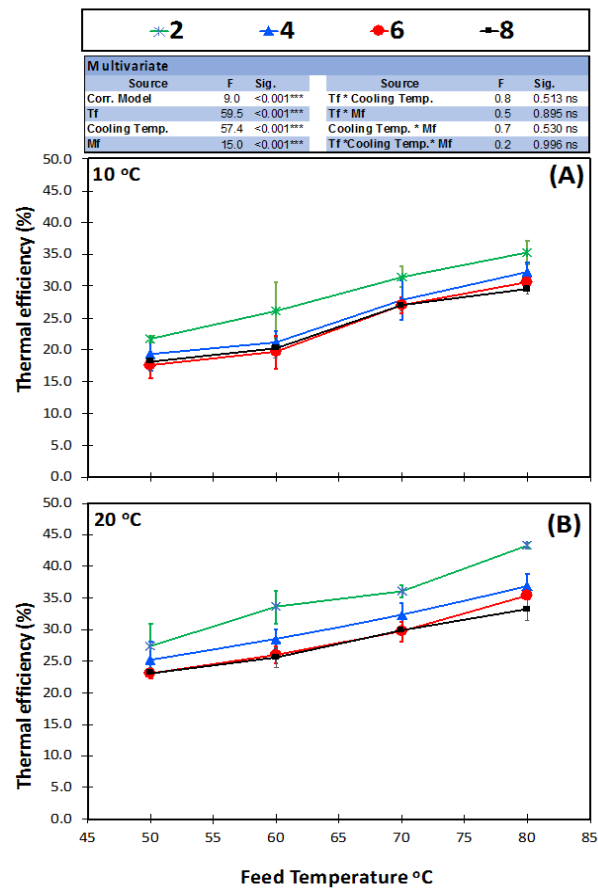


Fig. 3. The variation of thermal efficiency at different feed temperature ( $T_f$ ), feed flow rate ( $M_f$ ) and cooling temperature ( $T_c$ ).

Table 6. Analyses of variance (ANOVA) and multivariate analysis of thermal efficiency at different operating conditions

$T_f$ (°C)	$M_f$ (L/m)	Thermal efficiency ( $\eta$ )							
		10 °C				20 °C			
		Mean	SD	SEM	C.V.	Mean	SD	SEM	C.V.
50	2	21.68	0.96	0.55	4.41	27.32	6.27	3.62	22.94
	4	19.36	4.38	2.53	22.65	25.14	5.09	2.94	20.25
	6	17.55	3.39	1.96	19.32	22.98	1.38	0.79	5.99
	8	18.18	2.82	1.63	15.51	23.11	1.49	0.86	6.47
60	2	26.15	7.79	4.50	29.80	33.58	4.57	2.64	13.62
	4	21.22	3.01	1.74	14.20	28.47	2.62	1.51	9.20
	6	19.66	4.39	2.54	22.34	26.02	2.37	1.37	9.12
	8	20.28	2.75	1.59	13.57	25.59	2.74	1.58	10.70
70	2	31.45	2.89	1.67	9.18	36.07	1.61	0.93	4.48
	4	27.88	5.32	3.07	19.06	32.30	3.15	1.82	9.76
	6	26.99	2.14	1.24	7.94	29.71	2.71	1.57	9.13
	8	27.00	1.44	0.83	5.34	29.86	0.87	0.50	2.92
80	2	35.27	3.30	1.91	9.36	43.24	0.63	0.36	1.46
	4	32.17	2.61	1.51	8.11	36.85	3.36	1.94	9.13
	6	30.61	0.85	0.49	2.78	35.43	0.89	0.51	2.50
	8	29.51	1.20	0.69	4.06	33.24	3.24	1.87	9.76

NS; non-significant at  $p > 0.05$  \*, significant at  $p < 0.05$ ; \*\*, \*\*\* Highly significant at  $p < 0.01, 0.001$ .

Multivariate statistical analysis of evaporative latent heat transfer  $Q_{lh}$  (MJ/h) were presented in figure 4(A and B) and table (7). The main effect of temperatures  $T_f$  (50, 60, 70 and 80),  $M_f$  (2, 4, 6 and 8), and cooling temperature  $T_c$  (10 and 20 °C), and their interactions on evaporative latent heat transfer were evaluated at  $p < 0.05$  level.  $T_f$ ,  $M_f$ , and their interaction significantly changed evaporative latent heat transfer ( $F = 381.30^{***}, 263.8^{***}, 11.6^{***}$ ), respectively.

However, the effect of cooling temperature on evaporative latent heat transfer were non-significant ( $p > 0.05$ ).

Multivariate statistical analysis of energy flux  $Q_h$  (MJ/h) were presented in figure 5(A and B) and table (8).

The main effect of temperatures  $T_f$  (50, 60, 70 and 80 °C),  $M_f$  (2, 4, 6, 8), and cooling temperature  $T_c$  (10 and 20 °C), and their interactions on energy flux were evaluated at  $p < 0.05$  level.  $T_f$ ,  $M_f$ , cooling temperature interaction between  $T_f$ \*cooling temperature,  $T_f$ \* $M_f$ , cooling temperature\* $M_f$  were significantly changed energy flux ( $p < 0.001^{***}$ ). However, the interaction between  $T_f$ ,  $M_f$ , and cooling temperature on energy flux were non-significant ( $p > 0.05$ ).

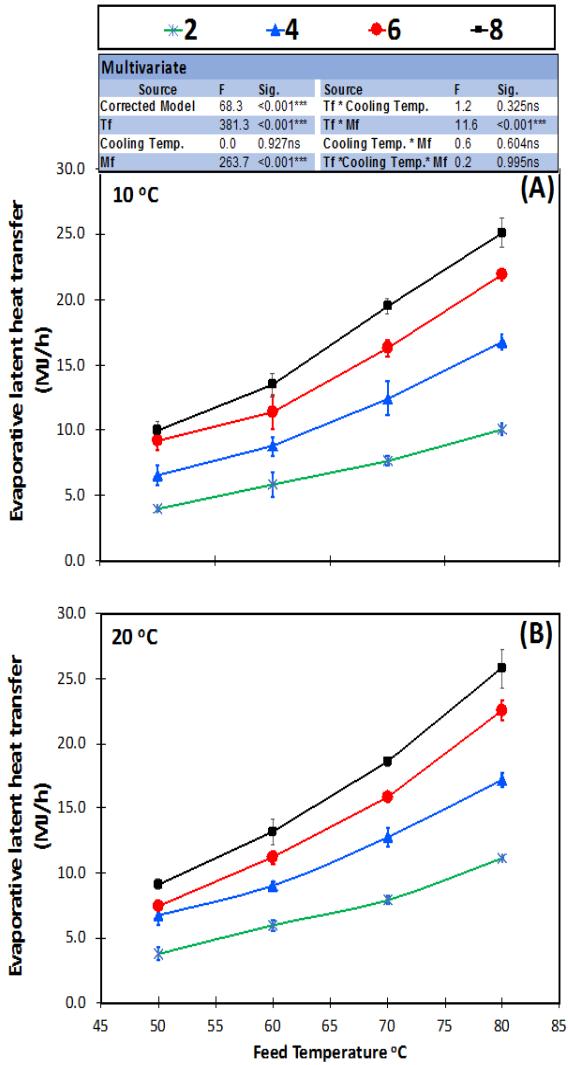


Fig. 4. The variation of evaporative latent heat transfer at different feed temperature ( $T_f$ ), feed flow rate ( $M_f$ ) and cooling temperature ( $T_c$ ).

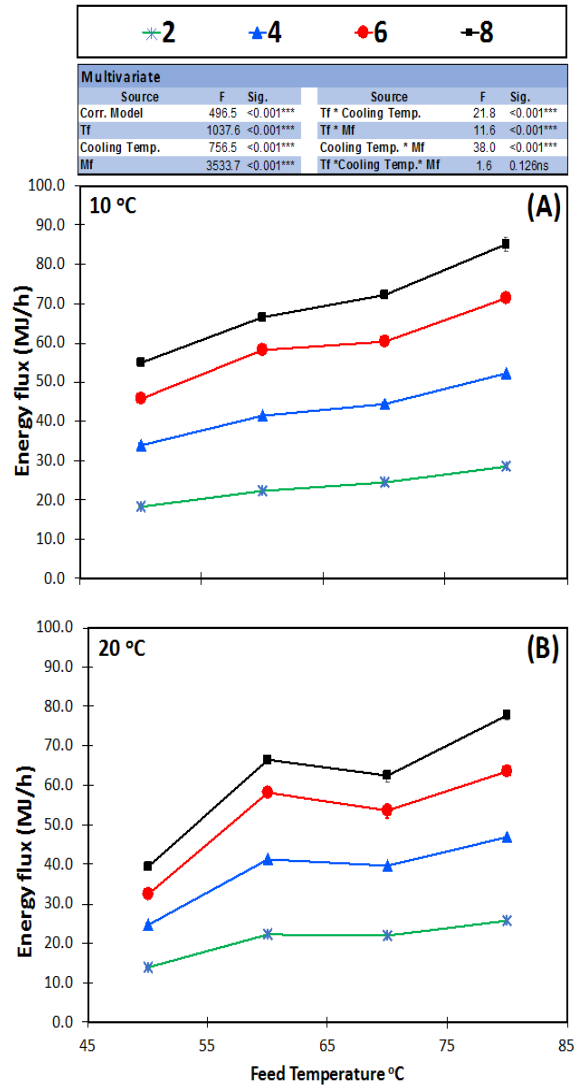


Fig. 5. The variation of energy flux at different feed temperature ( $T_f$ ), feed flow rate ( $M_f$ ) and cooling temperature ( $T_c$ ).

Table 7. Analyses of variance (ANOVA) and multivariate analysis of evaporative latent heat transfer at different operating conditions

$T_f$ (°C)	$M_f$ (L/m)	Evaporative latent heat transfer ( $Q_{Lh}$ )							
		10 °C				20 °C			
		Mean	SD	SEM	C.V.	Mean	SD	SEM	C.V.
50	2	3.95	0.26	0.15	6.54	1.62	0.38	0.22	23.15
	4	6.54	1.37	0.79	20.94	2.91	0.61	0.35	21.05
	6	9.21	1.27	0.73	13.75	3.20	0.18	0.10	5.49
	8	9.93	1.27	0.73	12.82	3.92	0.30	0.17	7.68
60	2	5.82	1.63	0.94	28.00	2.57	0.30	0.17	11.72
	4	8.77	1.24	0.72	14.15	3.89	0.20	0.12	5.12
	6	11.40	2.22	1.28	19.47	4.81	0.39	0.22	8.01
	8	13.47	1.56	0.90	11.57	5.66	0.73	0.42	12.92
70	2	7.65	0.61	0.35	7.96	3.40	0.22	0.13	6.41
	4	12.40	2.25	1.30	18.13	5.49	0.54	0.31	9.88
	6	16.28	1.12	0.65	6.89	6.81	0.29	0.17	4.21
	8	19.47	1.00	0.58	5.15	8.00	0.27	0.16	3.40
80	2	10.07	0.75	0.43	7.47	4.79	0.03	0.02	0.59
	4	16.77	1.02	0.59	6.10	7.40	0.41	0.24	5.55
	6	21.86	0.81	0.47	3.69	9.70	0.55	0.32	5.67
	8	25.12	1.86	1.07	7.41	11.10	1.12	0.64	10.06

NS; non-significant at  $p>0.05$  \*, significant at  $p<0.05$ ; \*\*, \*\*\*, Highly significant at  $p<0.01, 0.001$ .

**Table 8. Analyses of variance (ANOVA) and multivariate analysis of energy flux at different operating conditions**

T <sub>f</sub> (°C)	M <sub>f</sub> (L/m)	Energy flux (Q <sub>h</sub> )							
		10 °C				20 °C			
		Mean	SD	SEM	C.V.	Mean	SD	SEM	C.V.
50	2	5.33	0.97	0.56	18.13	13.79	0.26	0.15	1.88
	4	7.00	0.48	0.28	6.89	24.70	0.72	0.41	2.91
	6	8.37	0.43	0.25	5.15	32.42	1.68	0.97	5.19
	8	4.33	0.32	0.19	7.47	39.44	0.69	0.40	1.75
60	2	9.40	0.35	0.20	3.69	22.31	0.43	0.25	1.91
	4	10.80	0.80	0.46	7.41	41.33	0.46	0.26	1.10
	6	3.95	0.26	0.15	6.54	58.27	2.33	1.35	4.00
	8	6.54	1.37	0.79	20.94	66.53	1.31	0.75	1.96
70	2	9.93	1.27	0.73	12.82	21.91	0.50	0.29	2.27
	4	5.82	1.63	0.94	28.00	39.54	0.89	0.51	2.24
	6	8.77	1.24	0.72	14.15	53.49	3.10	1.79	5.81
	8	11.40	2.22	1.28	19.47	62.35	2.93	1.69	4.71
80	2	7.65	0.61	0.35	7.96	25.77	0.53	0.30	2.05
	4	12.40	2.25	1.30	18.13	46.81	1.73	1.00	3.69
	6	16.28	1.12	0.65	6.89	63.64	2.15	1.24	3.39
	8	19.47	1.00	0.58	5.15	77.69	1.99	1.15	2.56

NS; non-significant at p>0.05 \*, significant at p<0.05; \*\*, \*\*\* Highly significant at p<0.01, 0.001

### CONCLUSION

The performance of air gap membrane distillation (AGMD) module in terms of permeate flux (F<sub>p</sub>) and thermal efficiency (η) were investigated experimentally at School of Material Science and Engineering, Tiangong University, China. All data were described statistically in terms of means, standard error for means (SE), standard deviation (SD) and coefficient of variation (C.V.). Data were subjected to the analyses of the variance (ANOVA) and multivariate analysis to test the significant effect of different feed and designs at p<0.05. It was seen that the AGMD flux decreased largely with increasing cooling temperature from 10 to 20 °C. Whereas at M<sub>f</sub> of 2 and 4 L/m under T<sub>f</sub> of 50 °C, 6 and 8 L/m under T<sub>f</sub> of 50, 60 and 70 °C, the percentage of AGMD flux declined by about 4.71% (2 L/m), 4.98% (4 L/m), 7.51%, 1.84%, 2.71% (6 L/m), 8.20%, 2.25%, and 4.42% (8 L/m), respectively. On the contrary, at M<sub>f</sub> of 2 and 4 L/m under T<sub>f</sub> of 60, 70, and 80 °C, 6 and 8 L/m under T<sub>f</sub> of 80 °C, increasing T<sub>c</sub> from 10 to 20 °C improved AGMD flux. The percentage of AGMD flux (F) increased by about 2.80%, 3.34%, 14.78% (2 L/m), 3.18%, 3.00%, 2.64% (4 L/m), 3.19% (6 L/m), and 2.78% (8 L/m), respectively. Also, it was found that increasing T<sub>c</sub> from 10 to 20 °C upgraded meaningfully the thermal efficiency of AGMD module. The rate of increasing were as follows: 1.26, 1.29, 1.15, 1.27 times (2 L/m), 1.30, 1.32, 1.16, 1.14 times (4 L/m), 1.31, 1.33, 1.10, 1.15 times (6 L/m), and 1.27, 1.27, 1.11, 1.13 times (8 L/m) at different T<sub>f</sub> of 50, 60, 70 and 80 °C, respectively.

### ACKNOWLEDGMENTS

The authors would like to gratefully acknowledge the National Basic Research Program of China (No. 2015CB655303), the National Natural Science Foundation of China (No. 21076176), the National Key Technologies R&D Program (2015ZX07406006).

### REFERENCES

- Abu-Zeid, M. A. E. R., Zhang, L., Jin, W. Y., Feng, T., Wu, Y., Chen, H. L. & Hou, L. 2016. Improving the performance of the air gap membrane distillation process by using a supplementary vacuum pump. *Desalination*, 384, 31–42.
- Andersson, S. I., Kjellander, N. & Rodesjo, B. 1985. Design and field tests of a new membrane distillation desalination process. *Desalination*, 56, 345–354.
- Alklaibi, A. M. & Lior, N. 2004. Membrane-distillation desalination: status and potential. *Desalination*, 171, 2, 111–131.
- Alklaibi, A. M. & Lior, N. 2006. Heat and mass transfer resistance analysis of membrane distillation. *Journal of Membrane Science*, 282, 362–369.
- Alkhubhri, A., Darwish, N. & Hilal, N. 2013. Produced water treatment: Application of Air Gap Membrane Distillation. *Desalination*, 309, 46–51.
- Attia, H., Osmanb, M. S., Johnsona, D. J., Wrighta, C. & Hilal. N. 2017. Modelling of air gap membrane distillation and its application in heavy metals removal. *Desalination*, 424, 27–36.
- Aryapratama, R., Koo H., Jeong, S. & Lee, S. 2016. Performance evaluation of hollow fiber air gap membrane distillation module with multiple cooling channels. *Desalination*, 385, 58–68.
- Banat, F. 1994. Membrane distillation for desalination and removal of volatile organic compounds from water. Ph.D. Dissertation, McGill University, Montreal, Canada.
- Banat F. A. & Simandl, J. 1994. Theoretical and experimental study in membrane distillation. *Desalination*, 95, 39–52.
- Banat F. A. & Simandl, J. 1998. Desalination by membrane distillation: a parametric study. *Separ Sci Technol*, 33, 201–226.

- Carlsson, L. 1983. The new generation in sea water desalination: SU membrane distillation system. *Desalination*, 45, 221–222.
- El-Bourawi, M. S., Ding, Z., Ma, M. & Khayet, M. 2006. A framework for better understanding membrane distillation separation process. *Journal of Membrane Science*, 285, 4–29.
- Eykens, L., Reyns, T., De Sitter, K., Dotremont, C., Pinoy, L. & Van der Bruggen B. 2016. How to select a membrane distillation configuration? Process conditions and membrane influence unraveled. *Desalination*, 399, 105–115.
- Geng, H., Wu, H., Li, P. & He, Q. 2014. Study on a new air-gap membrane distillation module for desalination. *Desalination*, 334, 29–38.
- Khayet, M. 2013. Solar desalination by membrane distillation: dispersion in energy consumption analysis and water production costs (a review). *Desalination*, 308, 89–101.
- Khalifa, A. E., Alawad, S. M. & Antar, M. A. 2017. Parallel and series multistage air gap membrane distillation. *Desalination*, 417, 69–76.
- Khalifa, A. E. 2018. Performances of air gap and water gap MD desalination modules. *Water Practice & Technology*, 13, 1, 200–209.
- Khalifa, A. E. & Alawad, S. M. 2018. Air gap and water gap multistage membrane distillation for water Desalination. *Desalination*, 337, 175–183.
- MacInnes, J. 2017. An introduction to secondary data analysis with IBM SPSS statistics. Los Angeles: Sage Publications Ltd.
- O'Brien R. G. & Kaiser M. K. 1985. MANOVA method for analyzing repeated measures designs: An extensive primer. *Psychological Bulletin*, 97, 316–333.
- Pangarkar B. L. & Sane, M. G. 2011. Performance of Air Gap Membrane Distillation for Desalination of Ground Water and Seawater. *World Academy of Science, Engineering and Technology*, 5, 03–23.
- Roy, S. B., Chen, L., Girvetz, E. H., Maurer, E. P., Mills, W. B. & Grieb, T. M. 2012. Projecting water withdrawal and supply for future decades in the US under climate change scenarios. *Environ. Sci. Technol.*, 46, 2545–2556.
- Shatat, M., Worall, M. & Riffat, S. 2013. Opportunities for solar water desalination worldwide: Review. *Sustainable Cities and Society*, 9, 67–80.
- Swaminathan, J., Chung, H. W., Warsinger, D. M. & Lienhard, J. H. 2016. Membrane distillation model based on heat exchanger theory and configuration comparison. *Applied Energy*, 184, 491–505.

## تحلية المياه المملحة باستخدام وحدة تقطير غشائي ذو فجوة هوائية عند مستويين مختلفين لماء التبريد

مصطفى عبدالراضي أبو زيد<sup>1</sup> و شياولنج لو<sup>2</sup>

اقسم الهندسة الزراعية ، كلية الزراعة ، جامعة قناة السويس ، الاسماعيلية ، مصر  
<sup>2</sup> كلية علوم المادة والهندسة

أجري هذا العمل البحثي بهدف دراسة تأثير درجتي حرارة مختلفة لماء التبريد علي كلا من الإنتاجية والكفاءة الحرارية لوحدة تقطير غشائي ذو فجوة هوائية. تم وصف جميع البيانات المتحصل عليها إحصائياً من حيث حساب المتوسطات ، الخطأ القياسي ، الإنحراف القياسي ، معامل الاختلاف. وقد تم تحليل البيانات باستخدام كلا من تحليل التباين والتحليل متعدد المتغيرات وذلك لإختبار تأثير المعنوية لظروف التشغيل المختلفة عند  $p < 0.05$ . هذا وقد أجريت التجارب باستخدام مياه مملحة تصل درجة تركيز الأملاح فيها إلي 10000 مجم/لتر كمحلول مغذي عند درجات حرارة مختلفة للماء الساخن ومعدلات تدفق. أوضحت النتائج التجريبية المتحصل عليها أن إنتاجية وحدة التقطير الغشائي ذو الفجوة الهوائية قد إنخفضت بنسب مئوية مختلفة كما يلي: 4.71%، 4.98%، 7.51%، 4.42%، 2.25%، 8.20%، 2.71%، 1.84% وذلك عند زيادة درجة حرارة ماء التبريد من 10 إلي 20 م° علي التوالي عند معدلات تدفق 2، 4 لتر/رق (درجة حرارة مياة ساخنة تعادل 50 م°) و 6، 8 لتر/رق (درجات حرارة مياة ساخنة مختلفة تعادل 50 م°، 60 م°، 70 م°) ويرجع ذلك إلي إنخفاض فرق درجة الحرارة وفرق ضغط بخار الماء خلال الغشاء. علي الجانب الأخر فيما يتعلق بالكفاءة الحرارية لوحدة تقطير غشائي ذو فجوة هوائية ، فقد حصلنا علي نتيجة عكسية حيث زادت الكفاءة الحرارية عند زيادة درجة حرارة ماء التبريد من 10 إلي 20 م° عند جميع ظروف التشغيل المختلفة. حيث زادت الكفاءة الحرارية بمعدل 1.26، 1.27 مرة عند معدل تدفق 2 لتر/رق ودرجة حرارة مياة ساخنة مختلفة 50، 60، 70، 80 م° علي التوالي.